Analyst

Cite this: *Analyst*, 2012, **137**, 5803

www.rsc.org/analyst

**PAPER**

# Metal–organic framework templated synthesis of $Co_3O_4$ nanoparticles for direct glucose and $H_2O_2$ detection†

**Chuantao Hou, Qin Xu, Lina Yin and Xiaoya Hu***

***Received 12th July 2012, Accepted 11th October 2012***
**DOI: 10.1039/c2an35954e**



$Co_3O_4$ nanoparticles (NPs) with an average diameter of about 20 nm were synthesized by using MOFs as a template. Scanning electron microscopy (SEM) and transmission electron microscopy (TEM) were employed to characterize the as-prepared $Co_3O_4$ NPs. Fourier transform infrared spectroscopy (FT-IR) and X-ray diffraction (XRD) were used to confirm the structure of the $Co_3O_4$ NPs. Then the $Co_3O_4$ NPs were modified on a glassy carbon electrode (GCE) to obtain a non-enzymatic glucose and $H_2O_2$ sensor. The NPs show electrocatalytic activity toward oxidation of glucose and $H_2O_2$ in alkaline medium. For glucose detection, the developed sensor shows a short response time (less than 6 s), a high sensitivity of 520.7 μA $mM^{-1}$ $cm^{-2}$, a detection limit of 0.13 μM ($S/N = 3$), and good selectivity. The high concentration of NaCl does not poison the electrode. Its application for the detection of glucose in a human blood serum sample shows good agreement with the results obtained from the hospital. Furthermore, the proposed sensor was used for the detection of $H_2O_2$. The results indicate that the detection limit and sensitivity for $H_2O_2$ are 0.81 μM and 107.4 μA $mM^{-1}$ $cm^{-2}$, respectively. Determination of $H_2O_2$ concentration in a disinfectant sample by the proposed biosensor also showed satisfactory result. The high sensitivity and low detection limit can be attributed to the excellent electrocatalytic performance of the as-prepared $Co_3O_4$ NPs. These results demonstrate that the as-prepared $Co_3O_4$ NPs have great potential applications in the development of sensors for enzyme-free detection of glucose and $H_2O_2$.

## Introduction

Glucose and $H_2O_2$ detection is of critical importance in the fields of food, chemistry, biology, clinical control, and environmental protection.[1] Until now, many techniques including chemiluminescence electrochemistry, titrimetry, and spectrometry have been employed for the determination of $H_2O_2$ and glucose.[2] Among them, the electrochemical technique is a promising tool for the construction of simple, low-cost sensors owing to its high sensitivity, good selectivity and ease of operation. Enzymes have great potential for practical application and can be used for selective detection of glucose and $H_2O_2$. However, their inherent drawbacks, including easy denaturation by environmental changes, digestion by proteases, time-consuming and expensive preparation and purification, indeed limit their application for biosensors.[3] As a result, much effort has been devoted for developing non-enzymatic glucose and $H_2O_2$ sensors. In this respect, various functional materials such as noble metals, carbon nanotubes (CNTs), and metal oxides have been extensively investigated as the candidates for the development of effective enzyme-less sensors.[4] However, the sensors based on such materials suffer from either low sensitivity or poor selectivity towards the co-existed interfering species.[5] Recently, $Co_3O_4$-based electrochemical sensors have attracted considerable attention because of their excellent electrocatalytic performance toward glucose and $H_2O_2$ oxidation.[6] It is generally believed that the electrocatalytic performance of $Co_3O_4$ can be influenced by various factors such as size, surface-to-volume ratio, and level of crystallinity. Therefore, by adopting a specific synthetic approach, we can obtain nanoscale $Co_3O_4$ with excellent electrocatalytic performance toward glucose and $H_2O_2$ oxidation.

Metal–organic frameworks (MOFs) are a rapidly growing class of porous material with the remarkable characteristics of well-defined channels and cavities of regular size and shape that are easily tunable on the nanometer scale.[7] These fascinating properties of MOFs make them an ideal template for synthesizing nanoscale materials of various kinds such as silica nanoshells, nanoporous carbon, metallic nanoparticles and so forth.[8] Zeolitic imidazolic framework-8 (ZIF-8) is a chemically robust and thermally stable MOF material with ordered cavities of 11.6 Å, which can be used for synthesis of nanoscale metal oxides.[9] We expect that $Co_3O_4$ NPs synthesized by using ZIF-8 as a

*College of Chemistry and Chemical Engineering, Yangzhou University, Yangzhou, Jiangsu, China. E-mail: xyhu@yzu.edu.cn; Fax: +86-0514-87975244; Tel: +86-0514-87971818*

† Electronic supplementary information (ESI) available. See DOI: 10.1039/c2an35954e

template would have excellent electrocatalytic performance toward glucose and $H_2O_2$ oxidation.

In this work, $Co_3O_4$ NPs with uniform size distribution were obtained by using ZIF-8 as a template. Scanning electron microscopy (SEM), transmission electron microscopy (TEM), X-ray diffraction (XRD), and Fourier transform infrared spectroscopy (FT-IR) were applied to characterize the as-prepared sample. The $Co_3O_4$ NP modified glassy carbon electrode (GCE) shows excellent performance towards glucose and $H_2O_2$ detection in an alkaline medium. Our results prove that the as-prepared $Co_3O_4$ NPs have great potential applications in the development of sensors for enzyme-free detection of glucose and $H_2O_2$.

## Experimental

### Reagents

Zinc chloride, ammonium hydroxide, ammonium chloride, sodium hydroxide, sodium chloride, cobalt nitrate hexahydrate, glucose, and 30% $H_2O_2$ were purchased from Sinopharm Chemical Reagent Co. Ltd (Shanghai, China). 2-Methylimidazole was purchased from Aladdin Reagent Company (Shanghai, China). All other chemicals and reagents are of analytical grade and were used without purification. Real human serum samples were used without any sample pretreatment except a dilution step.

### Preparation of $Co_3O_4$ NPs

An existing approach was modified to synthesize $Co_3O_4$ NPs.[10] Briefly, a mixture of $ZnCl_2$ (0.808 g, 5.93 mmol), 2-methylimidazole (H-MeIM) (0.975 g, 11.88 mmol), and methane (80 mL) was heated at 100 °C for 4 h, and then cooled to room temperature. After removal of mother liquor from the mixture, colorless polyhedral crystals of ZIF-8 were obtained. They were washed with methane and evacuated at 200 °C before the next use.

$Co(NO_3)_2 \cdot 6H_2O$ was introduced into the ZIF-8 pores by the impregnation method. Typically, 0.1 g of ZIF-8 were dispersed in 10 mL of 0.6 g $Co(NO_3)_2 \cdot 6H_2O$ in ethanol and stirred at room temperature for 2 h. After being thoroughly washed with ethanol and water, the resulting powder was heated at 200 °C for 5 h (the composite obtained at this step was denoted as $Co_3O_4$@ZIF-8), and then to 600 °C for 5 h with a heating rate of 2 °C $min^{-1}$ in an air flow. The remaining powder was then dispersed in an $NH_4Cl$ (5 M)–$NH_3 \cdot H_2O$ (2.5 M) aqueous solution at room temperature to remove ZnO, which was formed from the decomposition of ZIF-8. The black $Co_3O_4$ NPs were washed several times with water and collected by centrifugation, finally dried at 100 °C overnight in an oven.

### Preparation of the $Co_3O_4$ NP modified GCE

To modify the electrode surface an aliquot of 5 μL of 1 mg $mL^{-1}$ as-synthesized $Co_3O_4$ NPs suspension in water was dropped onto the glassy carbon electrode (GCE) surface. After drying in air, the $Co_3O_4$ NP modified GCE was obtained.

### Apparatus and electrochemical measurements

A Hitachi S-4800 scanning electron microscope (Japan) was used to examine the morphology and the size of the surface of the as-synthesized $Co_3O_4$ samples. A TEM image was obtained with a Tecnai T12 transmission electron microscope operated at 120 kV. X-ray diffraction (XRD) patterns were recorded on a D8 Advance X-ray diffractometer (Bruker Co., Germany) at room temperature. FT-IR spectra were measured with a Tensor 27 spectrometer (Bruker Co., Germany). Electrochemical measurements were performed on a CHI 760D electrochemical workstation (Co., CHI, USA). All experiments were carried out with a three-electrode system with a glassy carbon electrode (GCE, $\varnothing = 3$ mm) as the working electrode, a platinum wire as the auxiliary electrode and a saturated calomel electrode (SCE) as a reference electrode. For amperometric detection all measurements were performed by applying an appropriate potential to the working electrode and allowing the transient background current decay to a steady-state value before the addition of the analyte. A stirred solution was employed to provide convective transport. All experiments were performed in compliance with relevant laws and institutional guidelines, and also approved by the institutional committees. Informed consent was obtained for any experimentation with human subjects.

## Results and discussion

### Characterization

A typical SEM image of the surface of the $Co_3O_4$ NP modified electrode is displayed in Fig. 1a. The size distribution of the $Co_3O_4$ NP is relatively uniform. The average diameter of the $Co_3O_4$ NP is about 20 nm, which is shown in the TEM image (Fig. 1b). It is worth noting that the diameter of the $Co_3O_4$ NP is much larger than that of the cavity of the ZIF-8 (1.16 nm), which corresponds to the results of Wang's work.[10] This phenomenon is attributed to the aggregation of cobalt precursor in the pores during the formation of $Co_3O_4$ upon heating.

The energy dispersive X-ray spectrum (EDX), which reveals the expected elemental constituents (*e.g.*, Co and O), shows no other impurities in the final $Co_3O_4$ NPs. The crystal structure and the phase purity of the as-synthesized $Co_3O_4$ NPs were further characterized by FT-IR and XRD. Fig. S1† shows the FT-IR spectrum of the as-prepared $Co_3O_4$ NPs. Two sharp peaks at 663 $cm^{-1}$ and 572 $cm^{-1}$ observed in the spectrum can be assigned to the stretching vibrations of the Co–O bonds existing in the Co(II,III) oxide.[11] The presence of $H_2O$ in the residue might be due to the moisture adsorption when it was exposed to air. Fig. S2† shows the XRD patterns of $Co_3O_4$ NPs (a) and $Co_3O_4$@ZnO (b) before dissolution of the zinc oxide. The XRD spectrum of

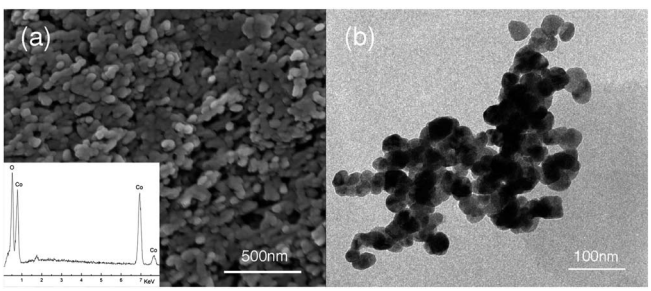


**Fig. 1** (a) SEM image of the surface of the $Co_3O_4$ NP modified GCE (inset of (a) was the EDX spectrum of $Co_3O_4$ NPs); (b) TEM image of the as-synthesized $Co_3O_4$ NPs.

$Co_3O_4$ NPs matches the standard spectrum of cubic crystalline $Co_3O_4$ (JCPDS 42-1467). The diffraction peaks at $2\theta$ values of 19.08°, 31.32°, 36.89°, 38.60°, 44.79°, 55.80°, 59.39°, 65.24°, and 74.09° correspond to (1 1 1), (2 2 0), (3 3 1), (2 2 2), (4 4 0), (4 2 2), (5 1 1), (4 4 0), and (6 2 0) crystal planes, respectively.[10] No other impurities could be detected in the XRD pattern of the as-synthesized $Co_3O_4$ NPs, indicating that $Co_3O_4$ NPs with high purity and high crystallinity are obtained.

### Electrochemical behavior of the $Co_3O_4$ NP modified GCE

As previously demonstrated, glucose detection with a $Co_3O_4$-based sensor is optimized in low-strength alkaline solutions.[6c] In our study, we also used NaOH solution as the electrolyte. Fig. 2 shows the cyclic voltammetric (CV) curves of the $Co_3O_4$ NP modified GCE in 0.1 M NaOH solution at different scan rates. In agreement with Ding's report,[6c] two pairs of redox peaks (I/IV and III/II) are observed, resulting from the reversible transition between $Co_3O_4$ and CoOOH (I/IV) and the transition between CoOOH and $CoO_2$ (III/II). These two reversible reactions can be schematically expressed as eqn (1) and (2):[12]

$$Co_3O_4 + OH^- + H_2O \leftrightarrow 3CoOOH + e^- \quad (1)$$

$$CoOOH + OH^- \leftrightarrow CoO_2 + H_2O + e^- \quad (2)$$

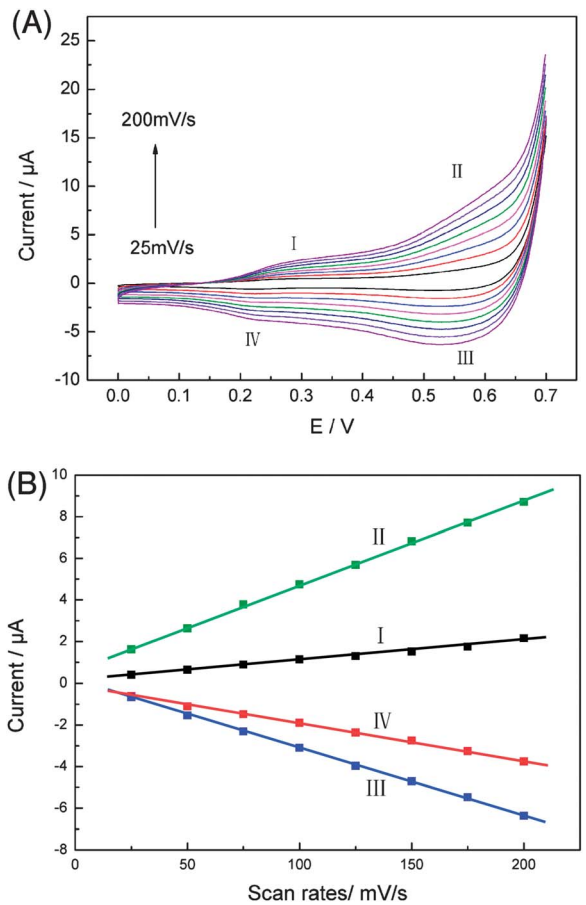


**Fig. 2** (A) CVs of the $Co_3O_4$ NP modified GCE in 0.1 M NaOH solution at various scan rates of 25, 50, 75, 100, 125, 150, 175, and 200 mV $s^{-1}$; (B) plot of peak currents *vs.* scan rate.

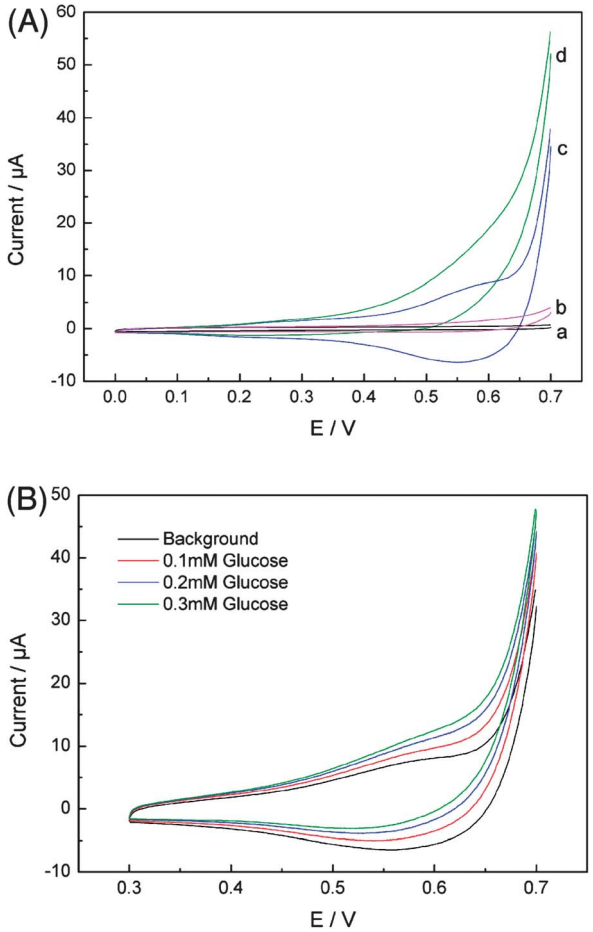


**Fig. 3** (A) CV responses of bare GCE in the absence (a) and presence (b) of 1.0 mM glucose and CV responses of the $Co_3O_4$ NP modified GCE in the absence (c) and presence (d) of 1.0 mM glucose; (B) CV responses of the $Co_3O_4$ NP modified GCE in the presence of various concentrations of glucose (0, 0.1, 0.2, and 0.3 mM). (Scan rate: 100 mV $s^{-1}$).

With an increase of the scan rate, both of the redox peak currents increase linearly with the scan rate in the range from 25 mV $s^{-1}$ to 200 mV $s^{-1}$, suggesting a surface-controlled electrochemical process.

### Electrooxidation behavior of glucose

Fig. 3A shows CV responses of the $Co_3O_4$ NP modified GCE in 0.1 M NaOH solution in the absence and presence of 1.0 mM glucose, at a scan rate of 100 mV $s^{-1}$ (for comparison purpose, experiments on the bare GCE under the same conditions were also carried out). It can be seen from the figure that there are no CV peaks for the bare GCE in the presence and absence of glucose. In contrast, there is a remarkable increase in the anodic current for the $Co_3O_4$ NP modified GCE after the addition of 1.0 mM glucose, with reference to the anodic peak current of the modified electrode before its addition. This increase is indicative of the excellent electrocatalytic activity of the $Co_3O_4$ NPs toward glucose oxidation. Careful observation indicates that the current increase with the addition of glucose at peak III (CoOOH → $CoO_2$) was much stronger than that at peak I ($Co_3O_4$ → CoOOH), which may

suggest that the electrooxidation of glucose is mainly mediated by $CoOOH/CoO_2$ rather than $Co_3O_4/CoOOH$ in an alkaline solution. Fig. 3B shows the CV responses of the $Co_3O_4$ NP modified GC electrode in 0.1 M NaOH solution containing various concentrations of glucose, *i.e.*, 0, 0.1, 0.2, and 0.3 mM. The apparent and linear increase in current at the potential of about +0.59 V (*vs.* SCE) indicates that the modified electrode can be applied for the detection of glucose with high sensitivity. Therefore, the peak III potential was applied for subsequent amperometric detection. It is widely accepted that glucose can be oxidized to produce gluconolactone through 2-electron electrochemical reaction.[4a] Therefore, as previously proposed,[6c] the mechanism of glucose electrochemical oxidation reaction catalyzed by $Co_3O_4$ NPs at peak III (+0.59 V) can be presumably depicted according to the following equation (eqn (3)):

$$2CoO_2 + C_6H_{12}O_6\ (\text{glucose}) \rightarrow 2CoOOH + C_6H_{10}O_6\ (\text{gluconolactone}) \quad (3)$$

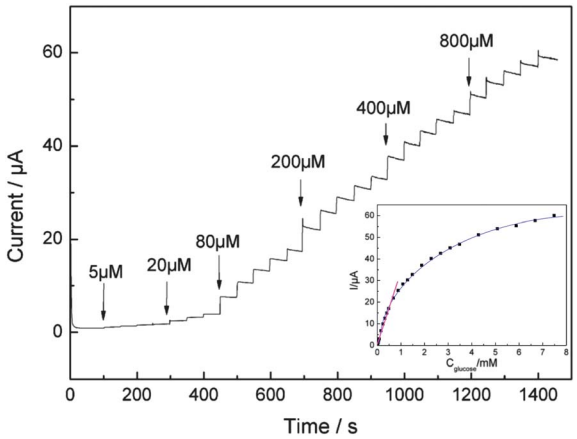


**Fig. 4** Amperometric response of the $Co_3O_4$ NP modified GCE on successive injection of the glucose solution of different concentrations into 0.1 M NaOH solution. Inset: calibration curve for current *vs.* concentration of glucose.

### Effect of NaOH concentration on glucose sensing

Since the $OH^-$ ion plays a significant role in the oxidation of cobalt oxide, the concentration of $OH^-$ ion in the electrolyte solution would have a great influence on the sensing performance of the $Co_3O_4$ NP modified GCE. The influence of the NaOH concentration on the amperometric detection of glucose was investigated. As shown in Fig. S3,† the optimal concentration of NaOH is 0.1 M for obtaining the best sensitivity for glucose.

### Amperometric detection of glucose

As the oxidation (anodic) peak current at *ca.* +0.59 V increases significantly with the increase of glucose concentration, an applied potential of +0.59 V (peak potential of peak III) was applied to conduct non-enzymatic amperometric detection of glucose in 0.1 M NaOH solution. Fig. 4 shows the typical amperometric response curves at the $Co_3O_4$ NP modified GCE on successive injection of glucose to the stirring NaOH solution. The proposed electrode achieved 95% of the steady-state current within 6 s, indicating a fast response time toward glucose detection on this sensor. The indicated concentration in Fig. 4 has considered the dilution effect. It is noteworthy that the slight baseline drift was observed after multiple injections of glucose, which may be attributed to a small variation of local pH, the faster glucose consumption than its diffusion, or the adsorption of intermediates on the active sites.[6c] The response increased linearly with the increase of glucose concentration ranging from $5 \times 10^{-6}$ M to $8 \times 10^{-4}$ M ($R^2 = 0.9939$) with a low detection limit of 0.13 μM ($S/N = 3$). The sensitivity for the $Co_3O_4$ NP modified GCE was calculated to be 520.7 μA $mM^{-1}$ $cm^{-2}$, which was higher than 1.06, 10.71, and 36.25 μA $mM^{-1}$ $cm^{-2}$ for the glucose electrochemical sensor based on single-walled carbon nanohorns,[13] platinum–gold alloy,[14] and $Co_3O_4$ nanofibers.[6c] In addition, the detection limit is among the lowest reported values for non-enzymatic glucose sensors.[4] The high sensitivity and low detection limit can be attributed to the excellent electrocatalytic performance of the as-prepared $Co_3O_4$ NPs. This result demonstrates that the $Co_3O_4$ NPs synthesized by using ZIF-8 as a template may have high specific surface area and numerous active sites which result in the excellent electrocatalytic property of the $Co_3O_4$ material.[10]

### Interference test and detection of glucose in serum samples

The selectivity of the $Co_3O_4$ NP modified GCE was also investigated against normally co-existed interfering species with glucose such as ascorbic acid (AA), uric acid (UA), and acetaminophen (AP). As the concentration of glucose in human blood is more than 10 times higher than those of the other three compounds,[15] the molar ratio of 1 : 10 was used for interferents in order to estimate their interference in the sensing of glucose. Fig. S4† shows the amperometric response of the $Co_3O_4$ NP modified GCE on successive injection of 0.2 mM glucose at different stages and for the addition of 0.02 mM UA, 0.02 mM AP, and 0.02 mM AA to the solution of 0.1 M NaOH, at an applied potential of +0.59 V. One can see that there is nearly no current response for 0.02 mM UA and 0.02 mM AP. Only 16% increase of amperometric response is observed for 0.02 mM AA compared to the response for 0.2 mM glucose; this current response is not significant. It is to be noted that glucose was added to the solution after each addition of the three interferents. The current response for each addition of glucose is still in a linear relationship, despite the additions of interferents. Such good selectivity against UA, AP and AA at +0.59 V may be contributing to the repelling effect between the negatively charged $Co_3O_4$ NPs and interferents in 0.1 M NaOH solution.[6c,d]

Since chloride ions can poison most of the non-enzymatic glucose sensors based on precious metals and alloys,[16] the influence of 0.1 M $Cl^-$ on the amperometric detection of glucose was investigated (Fig. S5†). It was found that there is nearly no current change between the amperometric responses for 0.2 mM glucose in the presence and absence of 0.1 M NaCl, implying that the $Co_3O_4$ NP modified GCE can work well for the sample with high concentration of chloride ions (*e.g.* blood sample).

In order to verify the above-mentioned reliability of the sensor, it was applied to detect the concentration of glucose in a human serum sample. The serum sample was analyzed by a OneTouch

 

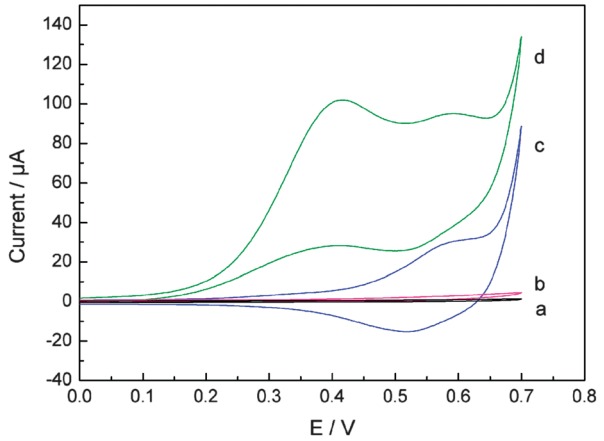


**Fig. 5** CV responses of bare GCE (a and b) and the $Co_3O_4$ NP modified GCE (c and d) in 0.1 M NaOH solution in the presence (b and d) and absence (a and c) of 1 mM $H_2O_2$.

Ultra glucose meter using glucose paper (Johnson and Johnson Medical Ltd., Shanghai, China) in the laboratory of clinical pathology division of a local hospital before our experiments. Fig. S6† demonstrated the amperometric response to successive two repeated additions of the glucose and serum sample in 0.1 M NaOH. The concentration of glucose in the human blood serum sample measured by our electrochemical method agrees well with that obtained in the hospital. The relative standard deviations (R.S.D.) are less than 5% for each serum sample, demonstrating good intra-electrode reproducibility. And then, we used correlation to compare the glucose meter method and our proposed method. The correlation coefficient between the two methods of six measurements is 0.77. These results imply the applicability of our $Co_3O_4$ NP modified GCE as a non-enzymatic sensor for the detection of glucose in human blood serum.

### Electrooxidation behavior of $H_2O_2$

In order to verify the electrocatalytic activity of the $Co_3O_4$ NP modified GCE for $H_2O_2$ oxidation, the electrochemical experiments in the presence of $H_2O_2$ were carried out. Fig. 5 shows cyclic voltammograms of the modified GCE and bare GCE in the absence and presence of 1 mM $H_2O_2$ in 0.1 M NaOH solution. As shown for bare GCE, no redox response of $H_2O_2$ can be seen in the potential range from 0 to 0.7 V (Fig. 5a). However, for the $Co_3O_4$ NP modified GCE, the oxidation current (peak I) related to $Co_3O_4$/CoOOH was greatly increased due to catalytic oxidation of $H_2O_2$ (Fig. 5d),[6e] indicating that the as-prepared $Co_3O_4$ NPs have high catalytic ability for $H_2O_2$ oxidation. The mechanism of the electrocatalysis can be shown by the following reactions:

$$6CoOOH + H_2O_2 \rightarrow 2Co_3O_4 + O_2 + 4H_2O \quad (4)$$

### Amperometric detection of $H_2O_2$

In order to evaluate the performance of the $Co_3O_4$ NP modified GCE toward $H_2O_2$ detection, an applied potential of +0.42 V ($Co_3O_4$/CoOOH) was applied to conduct non-enzymatic amperometric detection of $H_2O_2$. Fig. 6 displays the typical

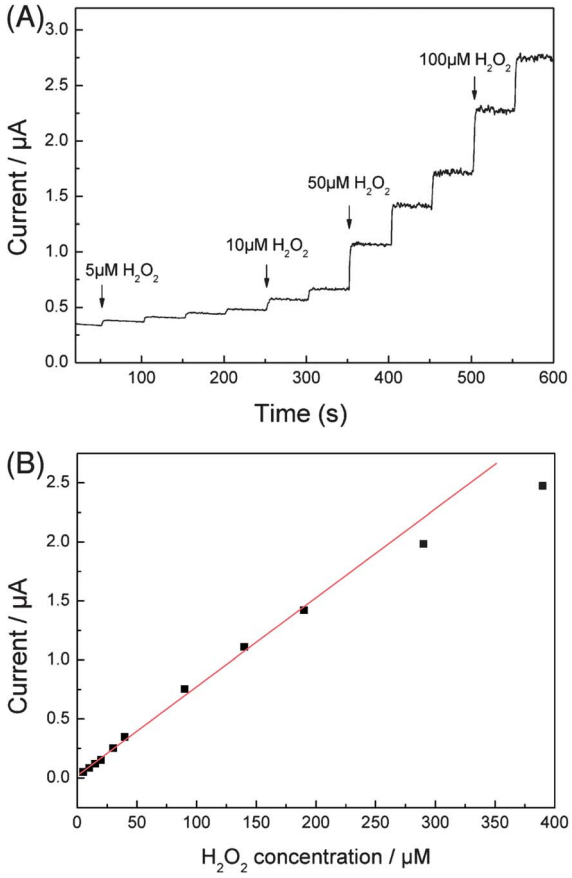


**Fig. 6** (A) Amperometric response of the $Co_3O_4$ NP modified GCE on successive injection of the $H_2O_2$ solution of different concentrations into 0.1 M NaOH solution. (B) Calibration curve for current *vs.* concentration of $H_2O_2$.

steady-state catalytic current–time response of the proposed GCE in 0.1 M NaOH with successive injection of $H_2O_2$ at an applied potential +0.42 V (*vs.* SCE). It can be seen from the calibration curve that the anodic current increases linearly with the increase of concentration of $H_2O_2$ up to 200 μM ($R^2$ = 0.9964). From the slope of the inset, the sensitivity of the $Co_3O_4$ NP modified GCE for $H_2O_2$ was determined to be 107.4 μA $mM^{-1}$ $cm^{-2}$. The detection limit was found to be 0.81 μM according to the sensitivity obtained from the calibration curve. Overall, the proposed sensor toward $H_2O_2$ detection has a higher sensitivity, a faster response speed, and a lower detection limit compared to the previously reported non-enzymatic sensors.[17]

**Table 1** Determination of $H_2O_2$ and the recovery test in a disinfectant sample

| Determined by potassium permanganate titration method[a] ($10^{-5}$ mol $L^{-1}$) | Added ($10^{-5}$ mol $L^{-1}$) | Determined by the proposed biosensor[a] ($10^{-5}$ mol $L^{-1}$) | Recovery (%) |
|---|---|---|---|
| 1.68 ± 0.22 | — | 1.63 ± 53 | — |
| | 2.0 | 3.71 ± 42 | 104 |
| | 4.0 | 5.69 ± 65 | 102 |
| | 6.0 | 7.56 ±73 | 99 |

[a] Average of five determinations ± standard deviation.

And then, the concentration of $H_2O_2$ in a disinfectant sample was determined by the proposed biosensor. The disinfectant sample was diluted with water, and the concentration of $H_2O_2$ contained in the diluted disinfectant sample was tested using the proposed biosensor. The result was compared with that obtained by the potassium permanganate titration (see Table 1). The recovery experiments were also performed. As shown, the result obtained by the proposed biosensor was in good agreement with this measured by the oxidation–reduction titration. The recovery rate was in the range 99–104%. These results indicated that it is feasible to apply the proposed electrode to determine $H_2O_2$ in real samples.

## Conclusions

In summary, $Co_3O_4$ NPs with an average diameter of about 20 nm were synthesized by using MOFs as a template, and subsequently modified on the GCE to obtain a non-enzymatic glucose and $H_2O_2$ sensor. To the best of our knowledge, this is the first report of direct detection of glucose and $H_2O_2$ by using a non-enzymatic electrochemical sensor. The $Co_3O_4$ NP modified GCE shows a broad linear sensing range, short response time, high sensitivity and low detection limit toward glucose and $H_2O_2$. For glucose detection, the proposed sensor has good selectivity against AP, UA, and AA. The amperometric detection of glucose in the serum sample implies the reliability of detection of glucose in human blood. This work demonstrates that the obtained $Co_3O_4$ NPs can serve as an ideal material for constructing fast, sensitive and stable amperometric sensors for the direct detection of glucose and $H_2O_2$. Since the size and morphology of the nanoscale $Co_3O_4$ can be tuned by adopting various MOFs with different cavities and channels, efforts are underway in our laboratory to construct $Co_3O_4$-based sensors with higher sensing performance toward glucose and $H_2O_2$.

## Acknowledgements

We gratefully acknowledge the financial support from the Natural Science Foundation of China (no. 21075107, no. 21275124, and no. 21275125) and the Educational Committee of Jiangsu Provincial General Universities Graduate Student Scientific Research Invention Plan (CXZZ12_0893). We also acknowledge the Project Funded by the Priority Academic Program Development (PAPD) of Jiangsu Higher Education Institutions.

## Notes and references

1 (*a*) Z. G. Zhu, L. Garcia-Gancedo, A. J. Flewitt, H. Q. Xie, F. Moussy and W. I. Milne, *Sensors*, 2012, **12**, 5996; (*b*) M. J. Whitcombe, I. Chianella, L. Larcombe, S. A. Piletsky, J. Noble, R. Porter and A. Horgan, *Chem. Soc. Rev.*, 2011, **40**, 1547; (*c*) L. Jiang and W. Zhang, *Electroanalysis*, 2009, **21**, 988.

2 (*a*) E. A. Moschou, B. V. Sharma, S. K. Deo and S. Daunert, *J. Fluoresc.*, 2004, **14**, 535; (*b*) K. Zargoosh, M. J. Chaichi, M. Shamsipur, S. Hossienkhani, S. Asghari and M. Qandalee, *Talanta*, 2012, **93**, 37; (*c*) B. S. Der and J. D. Dattelbaum, *Anal. Biochem.*, 2008, **375**, 132; (*d*) L. X. Cheng, S. Y. Deng, J. P. Lei and H. X. Ju, *Analyst*, 2012, **137**, 140.

3 (*a*) Y. Song, K. Qu, C. Zhao, J. Ren and X. Qu, *Adv. Mater.*, 2010, **22**, 2206; (*b*) E. Shoji and M. S. Freund, *J. Am. Chem. Soc.*, 2001, **123**, 3383; (*c*) Z. h. Dai, G. J. Shao, J. M. Hong, J. C. Bao and J. Shen, *Biosens. Bioelectron.*, 2009, **24**, 1286.

4 (*a*) S. Park, H. Boo and T. D. Chung, *Anal. Chim. Acta*, 2006, **556**, 46; (*b*) M. M. Rahman, A. J. Ahammad, J. H. Jin, S. J. Ahn and J. J. Lee, *Sensors*, 2010, **10**, 4855; (*c*) W. Siangproh, W. Dungchai, P. Rattanarat and O. Chailapakul, *Anal. Chim. Acta*, 2011, **690**, 10; (*d*) J. H. Lin, C. Y. He, Y. Zhao and S. S. Zhang, *Sens. Actuators, B*, 2009, **137**, 768.

5 W. Wang, L. Zhang, S. Tong, X. Li and W. Song, *Biosens. Bioelectron.*, 2009, **25**, 708.

6 (*a*) X. C. Dong, H. Xu, X. W. Wang, Y. X. Huang, M. B. Chan-Park, H. Zhang, L. H. Wang, W. Huang and P. Chen, *ACS Nano*, 2012, **6**, 3206; (*b*) X. W. Wang, X. C. Dong, Y. Q. Wen, C. M. Li, Q. H. Xiong and P. Chen, *Chem. Commun.*, 2012, **48**, 6490; (*c*) Y. Ding, Y. Wang, L. Su, M. Bellagambaa, H. Zhang and Y. Lei, *Biosens. Bioelectron.*, 2010, **26**, 542; (*d*) C. W. Kung, C. Y. Lin, Y. H. Lai, R. Vittal and K. C. Ho, *Biosens. Bioelectron.*, 2011, **27**, 125; (*e*) A. Salimi, R. Hallaj, S. Soltanian and H. Mamkhezri, *Anal. Chim. Acta*, 2007, **594**, 24; (*f*) C. W. Na, H. S. Woo, I. D. Kim and J. H. Lee, *Chem. Commun.*, 2011, **47**, 5148; (*g*) W. Z. Jia, M. Guo, Z. Zheng, T. Yu, E. G. Rodriguez, Y. Wang and Y. Lei, *J. Electroanal. Chem.*, 2009, **625**, 27.

7 (*a*) K. S. Park, Z. Ni, A. P. Cote, J. Y. Choi, R. Huang, F. J. Uribe-Romo, H. K. Chae, M. O'Keeffe and O. M. Yaghi, *Proc. Natl. Acad. Sci. U. S. A.*, 2006, **103**, 10186; (*b*) R. Banerjee, A. Phan, B. Wang, C. Knobler, H. Furukawa, M. O'Keeffe and O. M. Yaghi, *Science*, 2008, **319**, 939; (*c*) A. Phan, C. J. Doonan, F. J. Uribe-romo, C. B. Knobler, M. O'Keeffe and O. M. Yaghi, *Acc. Chem. Res.*, 2010, **43**, 58; (*d*) J. P. Zhang, Y. B. Zhang, J. B. Lin and X. M. Chen, *Chem. Rev.*, 2012, **112**, 1001.

8 (*a*) W. J. Rieter, K. M. Taylor and W. Lin, *J. Am. Chem. Soc.*, 2007, **129**, 9852; (*b*) H. L. Jiang, B. Liu, Y. Q. Lan, K. Kuratani, T. Akita, H. Shioyama, F. Zong and Q. Xu, *J. Am. Chem. Soc.*, 2011, **133**, 11854; (*c*) F. Schröder, D. Esken, M. Cokoja, M. W. E. van den Berg, O. I. Lebedev, G. Van Tendeloo, B. Walaszek, G. Buntkowsky, H. H. Limbach, B. Chaudret and R. A. Fischer, *J. Am. Chem. Soc.*, 2008, **130**, 6119.

9 (*a*) M. Müller, X. Zhang, Y. Wang and R. A. Fischer, *Chem. Commun.*, 2009, 119; (*b*) M. Müller, S. Hermes, K. Kähler, M. W. E. van den Berg, M. Muhler and R. A. Fischer, *Chem. Mater.*, 2008, **20**, 4576.

10 W. X. Wang, Y. W. Li, R. J. Zhang, D. H. He, H. L. Liu and S. J. Liao, *Catal. Commun.*, 2011, **12**, 875.

11 N. A. M. Barakat, M. S. Khil, F. A. Sheikh and H. Y. Kim, *J. Phys. Chem. C*, 2008, **112**, 12225.

12 I. G. Casella and M. Gatta, *J. Electroanal. Chem.*, 2002, **534**, 31.

13 X. Liu, L. Shi, W. Niu, H. Li and G. Xu, *Biosens. Bioelectron.*, 2008, **23**, 1887.

14 J. Ryua, K. Kima, H. S. Kimb, H. T. Hahnc and D. Lashmore, *Biosens. Bioelectron.*, 2010, **25**, 602.

15 E. Scavetta, B. Ballarin and D. Tonelli, *Electroanalysis*, 2010, **22**, 427.

16 (*a*) S. Park, T. D. Chung and H. C. Kim, *Anal. Chem.*, 2003, **75**, 3046; (*b*) S. Park, H. Boo and T. D. Chung, *Anal. Chim. Acta*, 2006, **556**, 46.

17 (*a*) W. B. Lu, Y. L. Luo, G. H. Chang and X. P. Sun, *Biosens. Bioelectron.*, 2011, **26**, 4791; (*b*) M. Han, S. L. Liu, J. C. Bao and Z. H. Dai, *Biosens. Bioelectron.*, 2012, **31**, 151.

 